Effects of the physical characteristics of foams on conditioned soil's flow behavior: A case study

Nour El Souwaissi, Irini Djeran-Maigre, Laurence Boulange, Jean-Luc Trottin

Manuscript (with Author details)

Effects of the physical characteristics of foams on conditioned soil's flow behavior: a case study

Nour EL SOUWAISSI[a,b,*], Irini DJERAN-MAIGRE[a], Laurence BOULANGE[b], Jean-Luc TROTTIN[b]

[a] Univ Lyon, INSA Lyon, GEOMAS, F-69621 Villeurbanne, France, nour.elsouwaissi@insa-lyon.fr, irini.djeran-maigre@insa-lyon.fr

[b] EIFFAGE Génie Civil, 78140 Vélizy-Villacoublay, France, nour.elsouwaissi@eiffage.com, laurence.boulange@eiffage.com, jean-luc.trottin@eiffage.com

* corresponding author

Abstract

Earth pressure balance shield (EPBS) is the excavation technique responding to the technical construction complexity of the future line 16-1 of the Grand Paris Express project. Its principle is based on the capacity of the excavated ground to transmit the forces needed to counterbalance the earth and water pressures of the working face. Additives are injected into the soil; on the cutting wheel, in the excavation chamber and/or in the screw conveyor. Their role is to assure the soil conditioning by modifying the soil's workability and its hydromechanical and rheological parameters. Therefore, the soil conditioning produces a plastic medium able to transmit the pressure to maintain the front face. In addition, as a second objective, the additives aim to overcome uncertainties in the soil.Depending on the case, the additives can reduce the clogging, internal friction, abrasiveness, and permeability of the soil. The additives can include water, surfactant, polymer and bentonite. The combination of water and surfactant with or without polymer produces the foam. In order to increase the excavation perfomance, laboratory prelimenary tests are performed to deduce the optimal foam parameters. Since no test measuring the foam characteristics is standardized yet, this article sums up the tests mostly used in foam characterisation; half-life measurements, rheological tests,

microstructural observations. As for the conditioned soil, slump test is frequently used by the tunnelling industry to recommend the optimal soil conditioning parameters in terms of workability. This test has been adapted in this study and the results are verified by rheological tests, then compared to the real foam injection data used for the project and their effect on mechanical parameters. For a specific type of excavated soil, the quality (type) of foam recommended by the laboratory work falls into the same choice of additive choice based on *in-situ* tunnelling excavation data. These findings are explained by the foams characteristics. Therefore, a correlation between foam and the conditioned soil (sandy soil with silt and low percentage of clay) with foam is deduced at different levels : micro, meso and macro (real) scales.

Keywords: earth pressure balance shield, foam, soil conditioning, flow behavior**,** microstructure, *in-situ*

1. Introduction

The urban population increase, followed by transportation problems, shows the need not to only construct subways but also to build them in an efficient way. In order to accelerate the excavation and enhance the security in highly dense urban areas, the conventional excavation techniques were developed to mechanical ones. The earth pressure balance machine took place in 1974 (Quebaud, 1996). The technique is based on the ability of the excavated soil, placed in the excavation chamber, to transfer the forces needed to counterbalance the earth and water pressures on the face of the machine. For these reasons, the earth pressure balance excavation technique was firstly used for fine grained soil. The advantage of this type of soil is its ability, by the addition of water when needed, to modify the soil consistency by building a plastic paste capable to transfer the required forces needed to stabilize the cutting face (AFTES, 2000). This texture is not common due to soil heterogeneity in most applications. In the case of soil with a high presence of clay, clogging problems on the cutting wheel will be induced (Ball et al., 2009, de Oliveira et al., 2019), as for a soil with high permeability, water spewing will be faced (Huang et al., 2019, Borio and Peila, 2010). Especially in such cases, the EPBS face stability can no longer be maintained, the soil needs to be treated. These uncertainties were overcome by combining tunneling and chemical industries, which leads to discover an effective way of

soil treatment known by soil conditioning. This type of soil treatment can be provided by the addition of additives in particular surfactants and/or polymers. The conditioning agent mostly used in soil conditioning by EPBS is foam that includes water, surfactants with or without polymers. The main role of foam is to change the soil hydro-mechanical and rheological parameters in order to meet the texture requirements for EPB machine. For general purpose, this is done by the presence of the foam bubbles that increase the pore volume of the soil-foam matrix, creating a more compressible material. In the case of clayey soil, the polymer is injected into the foam. They build a steric barrier that to avoid reagglomeration effect of clays. In the case of porous soil, there is a risk of segregation; water binding polymers can be used to dry out (liquid) soils.

Researchers tended to study foam characteristics related to foaminess, stability and rheology (Guillermic, 2011, Thewes and Budach, 2010, Denkov et al., 2020, EFNARC, 2005). Recently, microscopic studies had been performed to follow the foam bubble diameters (Wu et al., 2018, Tao et al., 2019) and to deduce the effect of polymers on the foam characteristics (Zhao et al., 2021; Li et al., 2022). Their results showed that the properties of the foam might significantly change in function of the parameters of its generation such as the type of foam generator, type of the conditioning agent, pressure, foaming agent concentration and foam expansion ratio.

Until now, no specific norm can be found to characterize the foam, but recommendations are given by researchers especially EFNARC (2005). However, there are still limited findings on the relationship between the foam characteristics and their ability to affect the soil microscopic and rheological parameters. In the framework of Grand Paris Express project, line 16-1, several foaming agents were used to meet the large need of soil conditioning among several tunneling machines. This paper sums up, in its first part, the foam tests mostly used in the tunnel industry and investigates the characteristics of two industrial foaming agents used on the Grand Paris Express project, line 16-1. It allows to deduce a correlation between the foam physical characteristics related to the presence or not of anti-clay polymer.

After revealing the foams aspects, the procedures of soil conditioning and the determination of the optimal soil-foam ratio take place. Some researchers have conducted well known tests on conditioned soil samples specifically slump test by a standard cone (Quebaud, 1996, Jancsecz et al., 1999, Vinai et

al., 2008, Peila et al., 2009, Thewes et al., 2010, Budach, 2011, Martinelli et al. 2017, Kim et al., 2021), rheology test by a rheometer or a viscometer, (Vennekötter, 2012, Galli, 2016, Freimann et al., 2018, Hu and Rostami, 2021), compressibility tests by the use of a Rowe cell (Psomas, 2001, Penaduarte, 2007) or a self-designed compression device (Budach 2011, Tao et al., 2019, Wang et al., 2021) and shear tests by the use of direct shear box apparatus or a self-designed shear test device (Psomas, 2001; Tao et al., 2019). On a larger scale, findings in this field were related for example to building a large-scale model of screw conveyor apparatus able to extract the spoil from a pressure chamber in a similar way as in EPBS (Vinai et al., 2008). The literature studies did not limit the conditioned soil characteristics investigations to the initial stage of foam injection, but also extended their researches to study the long-term evolution of the conditioned soil's hydro-mechanical characteristics in function of time (Djeran-Maigre et al., 2018, Carigi et al., 2020).

These findings rely on an important quantity of soil that is not always possible to provide at the beginning of the project or that can be not representative to the soil heterogeneity along the tunnel lining. Despite the previous research results, current practices show that trial and error is still adapted by pilots to inject foam into the excavating machine. This is due preliminary tests limitations, such as the non-taken into account of foam characteristics and soil heterogeneity in the preliminary laboratory and the difficulty of performing tests on conditioned soil under pressure, important to replicate the conditions of the excavation chamber. If the soil (for lab measurements) is not well selected, then the results in terms of the correlation between soil type and foaming agent will be distorted.

The first objective is to recommend a type of foaming agent for soil geology by linking between the foam physical characteristics, composition (related to the presence of anti-clay polymer) and the characteristics of soil (sandy soil with silt and low content clay in the case of this study). The second objective is to deduce, as a first approach, an interval of quantities of foaming agent to inject into the soil. This is done by a sequence of simple or quick known test methodologies (with low quantity of material) from the literature.

The type of foam and the first set of optimal foam parameters needed for a certain type of soil are deduced by the physical characteristics investigations of foams, the slump tests on soil-foams then verified by rheology tests and microstructural observations for soil-foams. Afterwards, the quantities

112 are compared to the real volume of foams injected by the EPB machine while excavating the future
113 line 16-1 of the Grand Paris Express project. The article is therefore not limited to the correlation
114 between the characteristics of foams but it also deduces the correlation between these characteristics
115 and the soil rheology at different scales. The physical characteristics of the foam and the flow behavior
116 of conditioned soil represent the micro and meso scales of the study. These results, deduced from
117 laboratory work, are compared to real excavation data that reflects the real scale of this study.

118 2. Case study: site description, soil and conditioning agents

119 The Parisian metro development is essential to follow up the current and future increase of population
120 expansion. In France, the Grand Paris Express is a project under construction, aiming to pursue the
121 population growth by creating 4 new metro lines of a 200 km in total: line 15, line 16, line 17 and line
122 18, in addition to the extension of the existing line 14. Among these lines, the future line 16-1 operated
123 by Eiffage Génie Civil will be our center of this study.
124

125 2.1 Site description

126 The work on line 16-1 consists on constructing 19.3 kilometers of tunnel, 18 ancillary structures and 5
127 stations. This tunnel will be excavated using several tunnel boring machines TBMs. The type of the
128 excavation machines depends on the type of soil to be excavated. An example of the geological
129 section encountered by a TBM of this future line of the Parisian metro, is shown on Figure 1. It can be
130 easily observed that three types of soil appeared on the TBM alignment: Calcaire Saint-Ouen (SO),
131 Sable de Beauchamp (SB) and Marnes et Caillasses (MC). Several surveys are performed to
132 characterize the soils; it shows an overall 'sandy – clayey' characteristics that require the use of earth
133 pressure balance machine excavation technique. For this project, 6 EPBSs having 3 different diameters
134 7.75 m, 8.92 m and 9.87 m, were chosen. These EPBSs launched progressively at the end of 2019 are
135 therefore in charge to excavate the line 16-1 with a high security and minimum settlement. Each of
136 them excavates at different proportions of soil types. The high excavation requirements need the
137 monitoring of the excavation parameters on short and long terms. For this reason, a TBM monitoring
138 software is installed in each EPBS. The software projects the following excavation data on the screens

: advance rate of the tunneling machine (mm/min), cutting wheel rotation (rpm), torque (kN.m) and energy of the cutting wheel (MJ/m^3), excavation chamber pressure (bar), foam and water injection volumes (l/m^3), screw conveyor rotation speed (kN.m), etc. Therefore, the parameters' instantaneous follow up is assured not only by the pilots located in the cabin but also by the technical responsables from their office. As for long term, at the end of each excavation ring, having a 1.5 to 2 m of length, the data is saved in the monitoring software system and can be extracted for further analysis. This point is detailled in paragraph 5. The parameters' values variations are directly linked to the characteristics of the encountered soil. The basic geological characteristics of the different type of soils must be known. In the following paragraph, the characteristics of the most common soil in the line are presented.

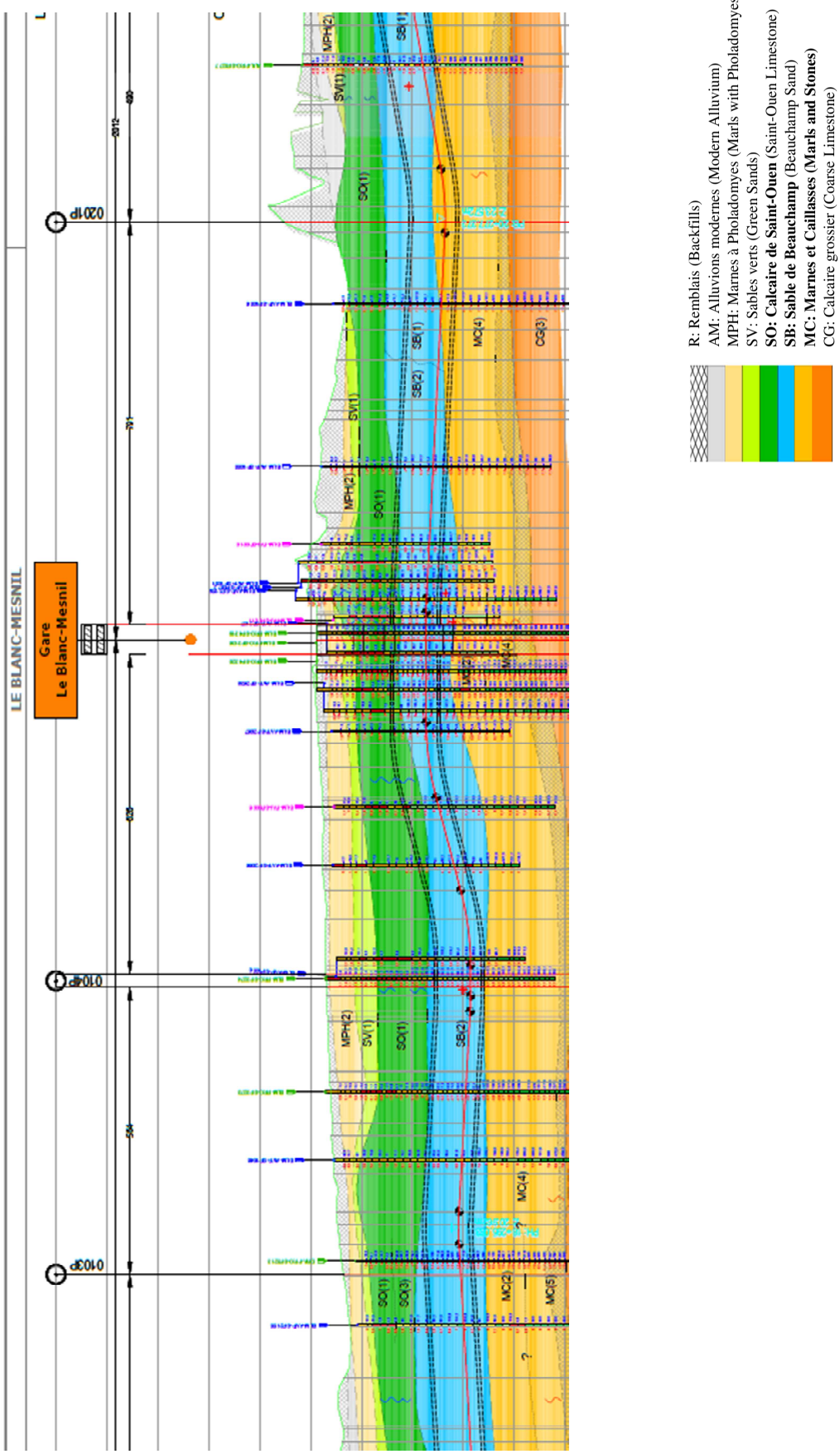

150

151 *Figure 1 : Geological section of line 16-1 alignment*

152 *(This figure must be in color)*

2.2 Soil

Among the different types of soil encountered in the project, Sable de Beauchamp, mostly faced by the tunneling machines, will be the highlight of the study. At the beginning of the project and before excavation takes place, Sable de Beauchamp soil samples are extracted from the site and then characterized in the laboratory of INSA Lyon. The particle size distribution of the soil is shown in Figure 2. The soil characteristics are summarized in Table 1.

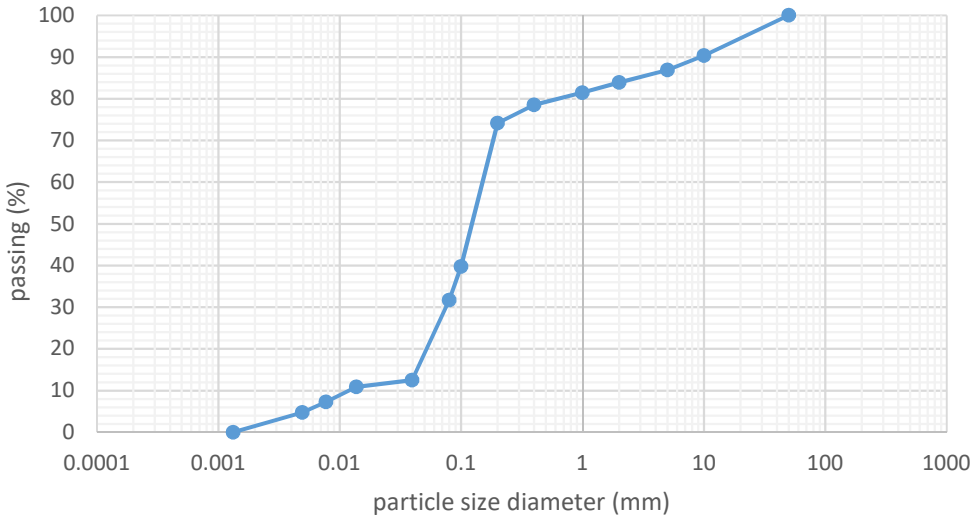

Figure 2: Particule size distribution of Sable de Beauchamp

The density of the soil taken into account is 2.1 Mg/m^3, this density is used to estimate the soil volume. The methylene blue value and plasticity index indicate a low clay percentage of the soil and subsequently a low adhesion tendency. According to the French classification GTR, this soil is classified as B5 (LCPC-SETRA, 2000). The comparison of the particle size distribution of Figure 2 with that shown in EFNARC (2005); Shi et al. (2021); Lovat (2012) indicates that the soil requires foam to improve workability and minimize the torque. Therefore, foam is injected on the cutting wheel of the machine, the excavation chamber and/or the screw conveyor, to increase the workability of the medium, which will ensure a sufficient flow of material in the excavation chamber and the screw conveyor, and therefore guarantees the safety of the excavation.

171 *Table 1 : Physical characteristics of the soil*

soil characteristics	Sable de Beauchamp
initial water content (%)	17
soil density (Mg/m^3)	2.1
passing 80 µm sieve (%)	31
methylene blue value	0.3
Liquid Limit	19
Plasticity Limit	12
Plasticity Index	7
consistency index	0.3

172

173 2.3 Conditioning agents

174 Due to the high demand on foam, several providers were chosen to sufficiently supply the six EPBSs.
175 Each foaming agent has its own composition that will have its own characteristics and will affect in a
176 specific way the microstructure of the soil. Due to the industrial confidentiality, no tests could be
177 performed to examine the chemical composition (presence or not of polymer) of the provided
178 materials. Based on the technical sheet, the conditioning agents used in this study are divided into two
179 categories; with or without anti-clay polymers. The first type of conditioning agent is symbolized by
180 "A", this type of additive has both surfactants and anti-clay polymers within his composition. The
181 second type of conditioning agent is given the name of "B", this agent is mainly formed from
182 surfactants and polymer with lubrication effect. The characteristics of both additives and their effects
183 on low clay content soil will be investigated within this study.

184 3. Foam characteristics

185 3.1 Parameters

186 Foam is a bubbly medium formed from the dispersion of gas into a liquid. It has been used for
187 different industrial purposes (Quebaud 1996): fire department (firefighting), cosmetics (shampoo,
188 razor gel…), beverages (beer...), petroleum (enhanced oil recovery), sanitary (soap…)…
189 Independently to its application domain, foam is mainly produced from three main components: water,
190 air and foaming agent based on surfactants (Figure 3). In the case of tunneling, surfactants have two
191 main roles: the first one is to modify the interface gas-water properties in order to create stable foam
192 bubbles and the second one, is to act on the soil grains once mixed with foam in a way to enhance the

soil characteristics. The amount of foaming agent, water and air to be incorporated into the foam are indicated by the following parameters:

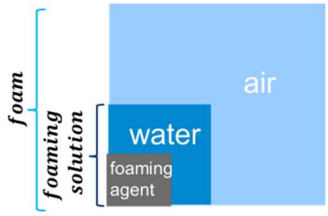

Figure 3 : Foam composition schema

- Surfactant concentration c_f (%), represents the amount of foaming agent in the foam

$$c_f(\%) = 100 * mass\ of\ the\ foaming\ agent\ /\ mass\ of\ the\ foaming\ solution \quad (1)$$

- Foam expansion ratio FER, characterizes the amount of air introduced into the foam

$$FER = volume\ of\ the\ foam\ /\ volume\ of\ the\ foaming\ solution \quad (2)$$

The transition from foaming solution to foam is based on air injection. This step can be assured by several techniques: foam generator or high-speed stirrer as defined by EFNARC (2005). The foam is generated by the use of a foam generator that functions as follow: In the first step, the water and the foaming agent are sent each at a specific flow. The flow is regulated in function of the desired c_f. These two foaming solution components are fed together with a stream of compressed air through a foam generator, which contains turbulators. The whirling and turbulent flow through the turbulators causes the foaming solution to foam. The foam is introduced into the existing support medium in the excavation chamber through openings in the cutting wheel, excavation chamber and screw conveyor, if needed (Thewes and Budach, 2010).

To generate the foam in this research, initially, the water is placed in a beaker, followed by the foaming agent, hence constituting the foaming solution. The high-speed stirrer of Rayneri brand is placed in contact with the foaming solution. It is switched on at 100 V, until the foam volume reaches

50% of the total desired volume. At this stage, the high-speed stirrer voltage is increased to 150 V. Once the foam volume reaches the total desired volume, the foam generation ends.

The foam characteristics highly depends on the type of foam generator and the pressure under which the foam is generated (Jancsecz et al. 1999, Thewes and Budach, 2010, Wu et al. 2018, Tao et al., 2019). The technique of generation by the use of a high-speed stirrer under atmospheric pressure is adapted in this research.

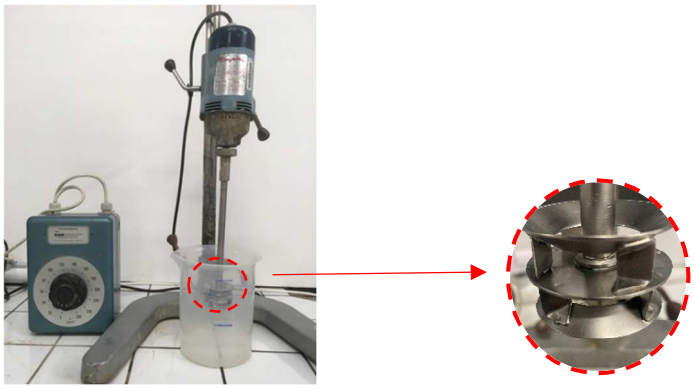

Figure 4: Foam generation in the laboratory

The concentration c_f was chosen equal to 1.5% and FER equal to 10; based on the mean recommended values by suppliers before the beginning of the excavation. These foam parameters values are refined in function of the results of tests performed on conditioned soil with foam.

Each foam generated at a specific concentration and expansion ratio has its own identity in terms of viscosity, life spans and bubble diameter. These mechanisms will be studied thoroughly in this article by the mean of several tests performed under atmospheric pressure: (i) density observation and half-life measurement to determine the stability of the foams, (ii) microstructure observation to follow the foam bubbles diameters, (iii) rheology test to determine the rheological behavior and the viscosity of each foam. The tests results allow deducing a correlation between the physical properties of foam and the presence or not of anti-clay polymer.

3.2 Foam stability

The generation and the life span of the foam are the result of several mechanisms that tend either to produce and stabilize this foam or to destroy it (Cantat et al., 2010). The mechanisms responsible of its

degradation are gravity, bubble coalescence and/or coarsening (Guillermic, 2011, Denkov et al., 2020, Wu et al., 2018). This paragraph describes the physical degradation of foam due to gravity by the use of two tests: evolution of foam density over time and measurement of foam's half-life.

3.2.1 Foam volume evolution

The aim of this method is to describe the physical degradation of the foam volume within time. The principal of the test is to follow the volume of foam placed in a closed cylinder in function of time. This method has been also used in Djeran-Maigre et al. (2018) and El Souwaissi et al. (2020). Initially, each of both foams is generated at $c_f = 1.5\%$ and $FER = 10$, placed in a covered 2 l cylinder having 8 cm of diameter and 54 cm of height. The volume evolution of each foam with time is captured by the use of a camera and the photos are reported on Figure 5. In the case of the foams used, 3 phases are distinguished while volume degradation. The first phase 'liquid', which is formed from the liquid drainage of foam due to the gravity effect, this phase is directly observed after few minutes from foam placement into the cylinder. The second phase 'dense phase' identified by small foam bubbles that gives a whitish color to the foam. The third and last phase 'light phase' where the foam bubbles are large enough, according a grey color to the foam. In the case of foam generated from foaming agent B, these three phases are easily distinguished. In this case, the volume of the dense phase is followed and reported on Figure 5 by the use of the equation (3). The method only follows the dense (white) phase of the foam since the foam lamellae adhere on the sides of the cylinder.

$$g(t) = \frac{V(t) - V_\infty}{V_0 - V_\infty} \qquad (3)$$

$g(t)$: temporal evolution relationship, $V(t)$: volume of foam at time t, V_0 : volume of foam at at=0

V_∞: volume of liquid foaming solution corresponding to zero change

However, in the case of foam generated from foaming agent A, the foam drains rapidly limiting the follow up of the evolution of the dense phase within the time.

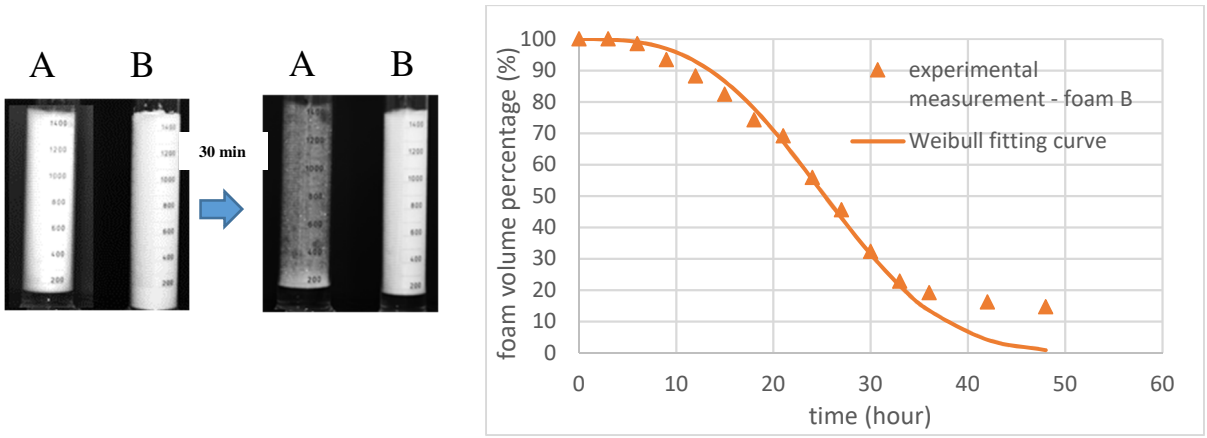

Figure 5 : Foam volume observation with time

The experimental points from the degradation of the foam B follows Weibull equation from t=0 to t=36h, with the following parameters: λ = 0.035 and β=3 :

$$g(t) = \exp\left[(-\lambda t)^{\beta}\right] \qquad (4)$$

Since the volume degradation data fits the Weibull equation, the half-life can be deduced by the use of the Weibull half-life function $(ln2)^{1/\beta}/\lambda$. The half-life of the foam in function of the volume degradation is equal to 25 hours. The foam degradation phenomena before mixing with the soil can be observed in standstill period related to maintenance, long ring installation… where the foam generator is filled by the foam. For this reason (among others), the foaming agent volume after a standstill is always higher than that injected during continuous excavation.

The same foaming product was used in previous work with different foam concentration and foam expansion ratio, results showed a similar degradation behavior with close values of λ and β. Therefore, for the same type of foam, despite the slight modification of the foam parameters, it will follow the same degradation behavior (exponential) with close parameters.

3.2.2 Half-life measurements from liquid drainage

The half-life parameter from liquid drainage indicates the time required to recover half of foaming solution mass, which was initially used to generate the foam. The method followed to measure the foam half-life is that described in EFNARC (2005): A mass of 80 g of foam generated from 2 different foaming agents is placed in a Pyrex™120mm Diameter Glass Büchner Filter Funnel. As shown on

Figure 6, the filter funnel is formed from an upper disc of 120 mm diameter and 1 l of capacity, a filter with pore size varying between 100 and 160 µm and a stem with 19 mm diameter and 120 mm height. Underneath the filter funnel, fixed on a tripod, a balance connected to a PC was placed. By this mean, the mass of the foaming solution resulted from foam drainage was collected and saved each 5 seconds. The mass of the foaming solution collected in function of time is shown on Figure 6:

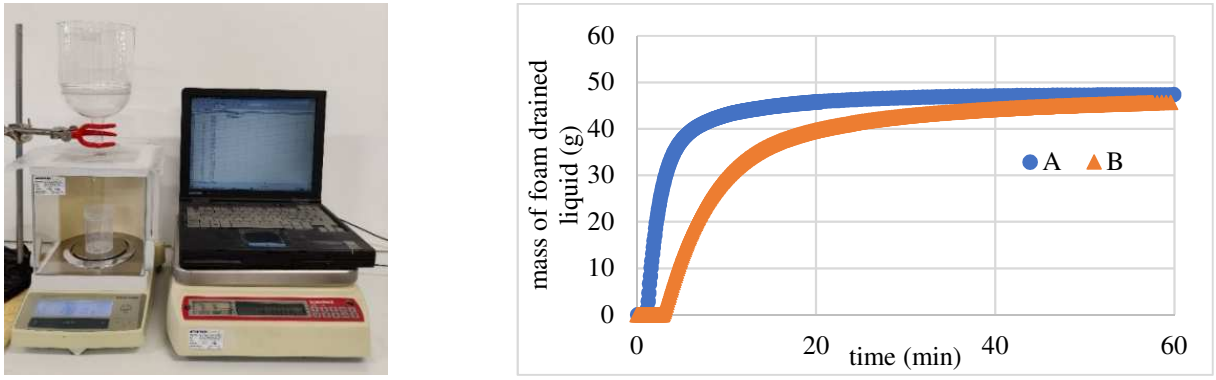

(a) (b)

Figure 6: Half-life measurements (a) filter funnel (b) variation of foam-drained liquid in function of time of two foaming agents

The foam half-life measurements are performed twice on each type of foam. Foam generated from the foaming agent A has a half-life equal to 6.8 ± 0.5 min, smaller than the half-life of foam generated from B, which is equal to 22.7 ± 2 min. By the use of the table of foam stability classification based on half-time (Sebastiani et al., 2019), foam generated from A is defined as a foam with moderate stability. As for foam generated from B, its half-life indicates that is highly stable. Since in most cases, the foam is directly injected into the soil, this criterion does not give a preference of foaming agent.

In general, both tests showed that foaming agent B is more stable (higher half-time value) than A. In the first method, the liquid is quickly drained and the foam volume was followed; in the second test, this liquid drained velocity was quantified. The two foam stability techniques do not determine the same meaning of half-life. However, both stability measurement techniques give the same result as stability tendency.

3.3 Rheological parameters

The rheological parameters of the foam, in particular its viscosity, shear stress and their evolution with the shear rate, are newly introduced in the case of foam studied in EPBS. In this study, the rheological tests on foams were conducted by the use of an Anton Paar rheometer MCR52 having a Peltier cooling system. This system allows maintaining the temperature while performing the test in order to eliminate any temperature effect. The tool used is the coaxial cylinder CC27 with a corresponding cup of a 26.7 mm diameter. The steps performed to conduct the tests are resumed as follow: Both foams are generated with the following parameters c_f = 1.5% and FER = 10. Then, 25 ml of the generated foam is placed in a CC27 and tested under a logarithmic ramp profile with shear rate increasing from 1 to 500 s^{-1}. In order to avoid the degradation mechanism of foam within the test, each second a measurement is recorded, which lead to limit the duration of the test to 100 s. The test is conducted at 20°C. The flow and viscosity curves of foams are shown on Figure 7.

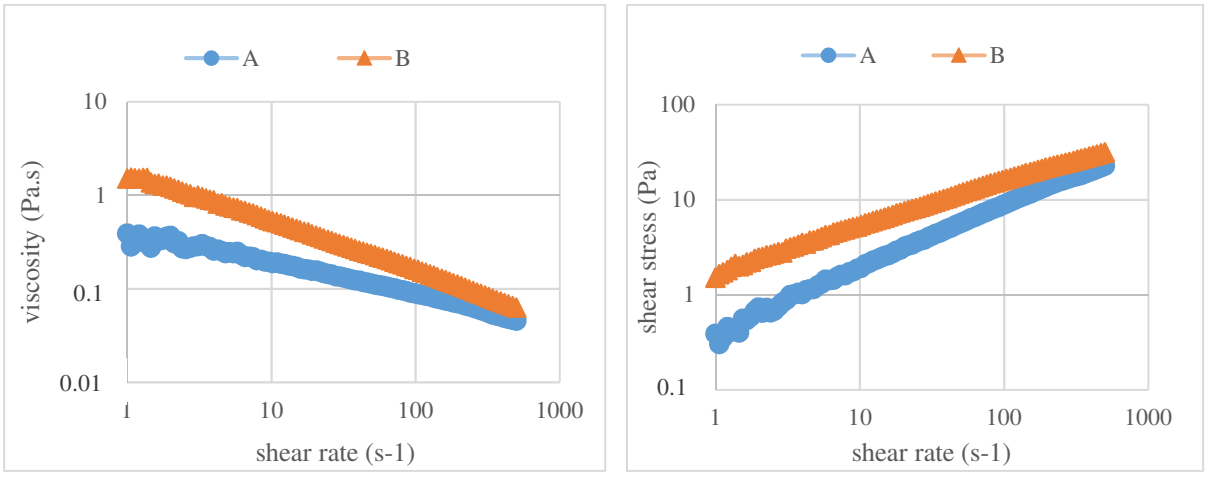

(a) (b)

Figure 7 : Characterization of the viscosity of the foam a) shear stress versus shear rate b) viscosity versus shear rate

By comparing the results, two categories of foam viscosities are distinguished. The first category is the one including foam A with low viscosity compared to the viscosity of foam B, the second category is the higher viscosity of foam B. Independently of these differences, both foams have a similar flow behavior: the shear stress of both foams increases when the shear rate increases, the viscosity decreases with the shear rate. This behavior also known as pseudo-plastic flow behavior indicates that

316 each of the two foams is a shear-thinning fluid. It can be explained by the destruction of the air
317 bubbles of foams and the films between them while resisting to the shear movement.

318 3.4 Microstructural observations

319 The objective of the microstructural study on foams is to correlate the bubble size with the physical
320 characteristics of the foam. In the case of this study, microscope ZEISS (Axio Imager M2m) is used to
321 follow the microstructural behavior of the foam. It can zoom between 25 to 500 times and transfer the
322 light in two ways: reflection mode or transmission mode throughout the sample.
323 The protocol adapted is initially based on generating each foam at c_f = 1.5% and FER = 10, then
324 placing it in 1 mm thickness tube with a lamella on the top. This structure is then positioned under the
325 microscope functioning at 25x zoom with light transmission mode. By the use of AxioVision software,
326 foam microscope images are visualized, recorded with elapsed time of 15 s for 60 min and then
327 analyzed. The data analysis is based on measuring the bubbles diameters, dividing them into intervals
328 and representing them on a histogram. This protocol was performed on both foams, each generated at
329 c_f = 1.5% and FER = 10. Only photos captured at initial stage (t=0) are analyzed in this study.

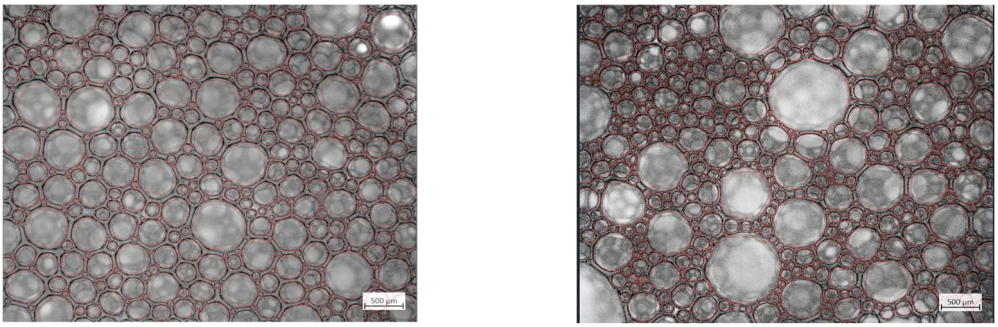

(a) Foam A (b) Foam B

330

331 *Figure 8 : Foam bubbles at t=0 for (a) foam A (b) foam B*

332 Visually the photos captured at t=0 (Figure 8), showed that foam A has more uniform bubbles,
333 whereas the foam B has some large bubbles but an overall are smaller ones. In order to quantify these
334 results, bubble's diameters are measured and divided into intervals: (0.05-0.15), (0.15-0.25), (0.25-
335 0.35), (0.35-0.45), (0.45-0.55) mm. Larger foam diameter bubbles are taken in the counting but not
336 presented The mean bubble diameter of foam A is equal to 195 µm, higher than the mean bubble

diameter of foam B equal to 178 µm. The number of bubbles of foams generated from foaming agents A and B is respectively: 372 - 435 bubbles for a surface of 5350 x 4250 µm.

The percentage of foam bubbles' diameters in function of the diameters interval is shown, for each foam, on the histogram (Figure 9). A similar method of analysis was performed by Tao et al. (2019).

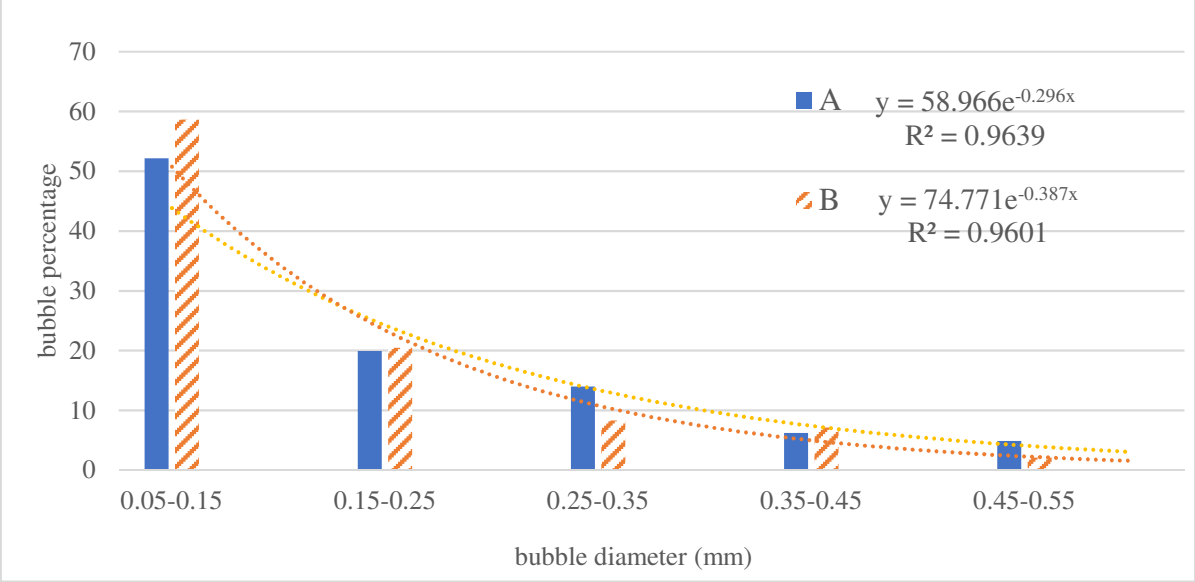

Figure 9: Bubble percentage distribution in function of bubble diameter

The main conclusions are summarized as follow:

- percentage distributions of bubbles for both foams follow an exponential equation

$$f(x) = \alpha \exp(-\lambda x)$$

  with different parameters:

  foam A: y = 58.996exp.(-0.296x) with $R^2 = 0.9639$

  foam B: y = 74.771exp.(-0.387x) with $R^2 = 0.9601$.

  The x is equal to 20 multiplied by the mean value of each class minus 1.

- two categories of foam's bubble diameters are distinguished: case B with smaller diameter and number of bubbles, yet more dispersed; and case A with bigger and more uniform bubble size. This indicates that the foam B has lower diameter bubbles that can fit into the same volume cylinder in comparison to foam A. Therefore, the smaller and more heterogeneous bubbles of foam B, create a longer drainage path than foam A.

4. Soil foam tests

The foaming agent type and quantity to inject into the soil should be chosen carefully. The effect of foam on the soil is a main concern since it highly depends on both characteristics of soil and foam. In order to provide a first approach for the optimal foam parameters to inject into the soil, slump tests are performed. The study is followed by rheological test and microstructure analysis performed under atmospheric pressure aiming to (i) quantify the flow behavior by calculating its viscosity and (ii) deduce the distribution of foam bubbles into the soil. The physical characteristics of foams determined from the first part, associated to the optimal foam parameters and the soil-foam microstructure allow correlating between the foam's physical characteristics and the soil properties.

4.1 Flow behavior approach

4.1.1 Slump test

The slump test by the use of the standard cone is highly used by the tunneling industry due to its advantages as a quick and easy index test able to give a general idea of the optimal soil workability for EPBS excavation. However, the slump test has limitations that is related to the fact that it gives qualitative results of workability. In addition, the slump has limitations such as the incapacity to detect the clogging potential of clayey soil and incapacity to measure the water permeability when used for the cohesionless soil. The protocol followed to perform the slump test on conditioned soil is mainly that adapted for the concrete (ASTM C143/C143M). The norm consists into pouring three layers of sample while compacting each. The cone is then lifted and the slump is measured. In the case of conditioned soil samples, an important number of researchers avoids the compacting step in order not to disturb the foam bubbles. The suitable range of slump for adequate workability of the support medium in an EPBM varied broadly between 100 and 250 mm. For example, Peila et al. (2009) performed slump tests on various types of cohesionless soil without compacting the sample, the optimal slump in their research varied between 140 and 200 mm. Vinai et al. (2008) performed slump tests on medium-grain sands with varying amounts of silt without samples compacting and for their work, the optimal slump value varies between about 150–200 mm. Quebaud (1996) followed the exact

methodology of performing slump test on concrete by compacting the conditioned soil, aiming to an optimal slump value of 120 mm. Jancsecz et al. (1999) did not explain the protocol followed for slump test, but suggested a suitable slump value between 200–250 mm. Martinelli et al. (2017) performed slump tests on granular conditioned soils. The slump fall ranging from 15 to 25 cm was used as reference value in their research. Peron and Marcheselli (1994) performed slump tests on gravel sand. They aimed for slump between 5 and 15 cm. Williamson et al. (1999) performed slump test for granular soils with fines and coarse grained soils. They suggested a slump value of 210 mm. In the case of Boone et al. (2005) the material amounts were adjusted to obtain a slump of between 8 and 10 cm in the case of soil consisting of gravel, sand, and cobbles.

Wei et al. (2020) performed slump tests on clay-sand-gravel mixed while compacting. They aimed for slump between 100 and 200 mm. This high variability of optimal slump values depends on the type of soil and the foam injection ratio. It can also be noticed that researches who performed slump tests while soil compacting recommended a smaller slump value in comparison to those who did not compact the samples. Unfortunately, this point cannot be assured since a large number of researchers did not share their slump test protocol.

In order to recommend the optimum foam-soil parameters, the procedure followed in this research is based on performing slump test on conditioned soil with various Foam Injection Ratio FIR (%).

$$FIR\ (\%) = 100 * \ volume\ of\ foam\ /\ volume\ of\ in\ situ\ soil\ to\ be\ excavated \quad (4)$$

The first step of the protocol consists on preparing the soil. The soil used is the Sable de Beauchamp with a water content maintained to its initial value $17 \pm 0.5\%$ that excludes the influence of water content on soil flow behavior. The similarity in the type the Sable de Beauchamp used is verified by performing methylene blue value measurements on several samples and by checking the texture of the soil (color and water content).

The second step consists on foam generating by the use of a high-speed stirrer. Directly after foam generation comes the third step that includes soil-foam mixture at various ratio by the use of a concrete mixer. In the last step, conditioned soil is immediately poured into the standard cone, lifted and the slump value is measured. For these types of tests, the samples are not compacted once placed into the cone in order not to disturb the bubbles. By the use of this protocol, two series of tests, each

409 with a different foaming agent, are performed. Due to the high volume required to conduct a slump
410 test, one to two tests per FIR are performed. The results showing an increase of the slump value as a
411 function of FIR, are the mean to validate each measurement. The first series of tests are conducted on
412 the soil conditioned with foaming agent A, generated at c_f = 1.5% and FER = 10, then mixed with the
413 soil at FIR = 30%, 40%, 45%, 50%, 60% and 70%. The slump tests (Figure 10) show an increase in
414 the slump values with the increase of foam injection ratio, which reveal the effectiveness of the foam
415 A on the studied soil. The slump increase is less significant at *FIR*=45%. This indicates that at this
416 point the soil-foam matrix is saturated with foam.

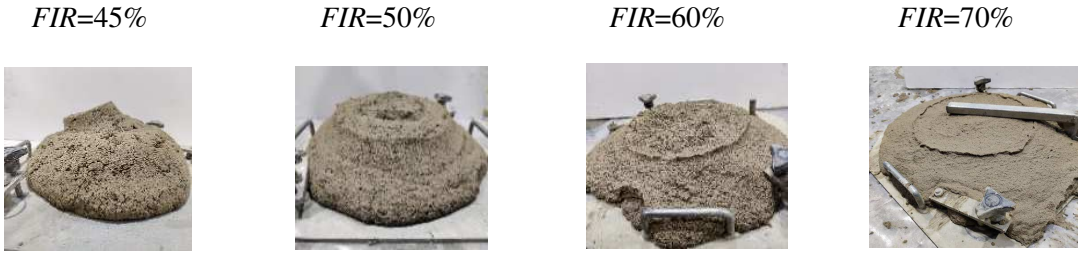

417 *Figure 10 : Slump variation in function of FIR in the case of conditioned soil with foam A, generated*
418 *at cf=1.5% - FER=10*

419
420 A second series of tests are also conducted on conditioned soil samples consisted from Sable de
421 Beauchamp mixed with foaming agent B, generated at c_f = 1.5%, FER = 10, at FIR = 45 – 60%. In
422 the case of FIR = 45%, the texture of the conditioned soil was dry and no slump was recorded. In the
423 case of FIR = 60 % a small slump of 67 mm was obtained (Figure 11 (a)).

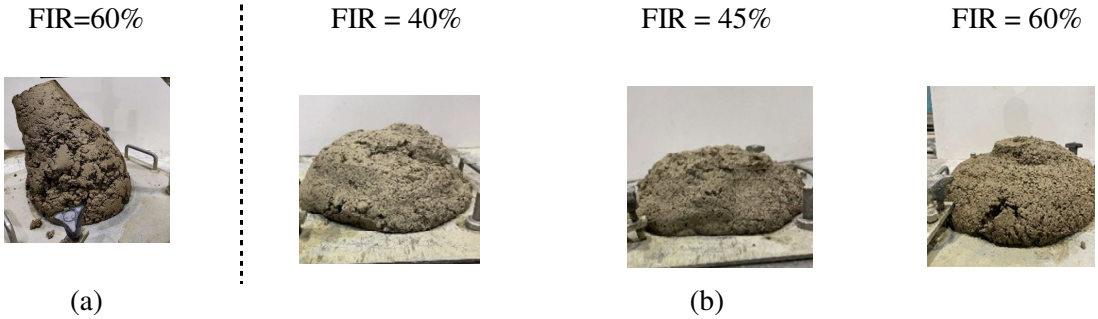

424 *Figure 11 : Slump tests at various FIR in the case of foaming agent B generated at: (a) cf=1.5% -*
425 *FER=10 (b) cf=2% - FER=8*

426 The results indicate the exigency of foam parameters modifications. The c_f is increased to 2% and the
427 FER is decreased to 8 in order to generate more dense foam. With these new parameters, foam B is

generated and mixed with the soil at different injection ratios: 40% – 45% and 60%. The increase of FIR from 40% to 60% slightly increased the slump values (Figure 11 (b)). The results show more adequate flow behavior to the EPBS.

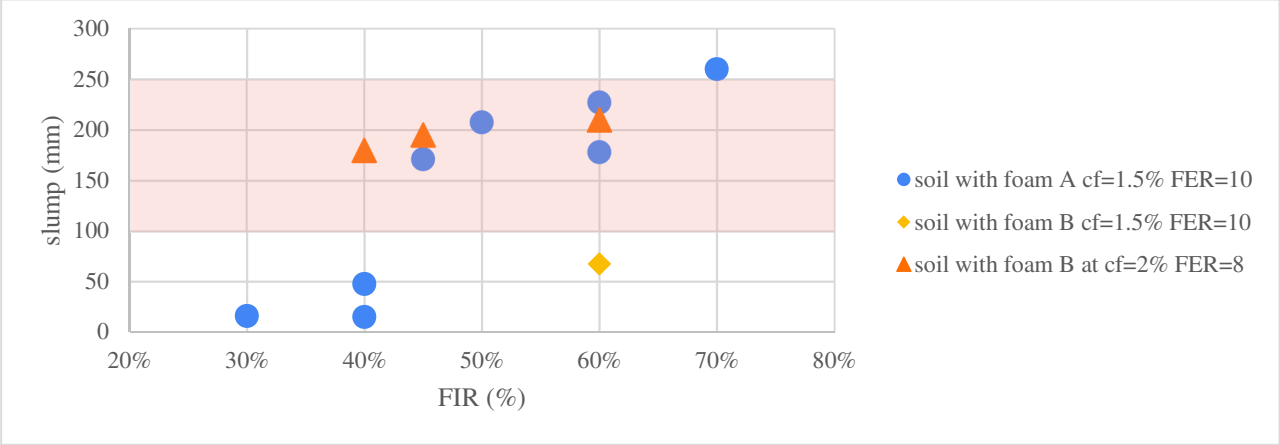

Figure 12 : Slump in function of FIR variation

As mentioned previously, the upper and lower limits of slump for optimal conditioned soil texture are considered between 100 and 250 mm. These values are highlighted on Figure 12. Consequently, in the case of foaming agent A, the recommended foam parameters based on slump tests are c_f = 1.5% - FER = 10 and FIR = 45-60%. In order to fulfill the soil texture requirements for EPB machine, the foaming agent B is recommended to be generated at c_f = 2%, FER=8 and mixed with the soil at FIR = 40-60%.

4.1.2 Rheological parameters

The rheological test by the use of the rheometer has an advantage over the slump test as its capacity, with a small quantity of soil, to measure the rheological parameters: viscosity, shear stress allowing to deduce the yield stress. In the case of this study, the aim of the rheological test is to verify the effect of the foam on the flow behavior of the soil and to deduce the optimal viscosity value. The rheological tests are performed by the use of Anton Paar MCR52 rheometer with a plate-plate system having a rough surface, which reduces the wall slip effect. The advantage of this method is related to the small volume required to conduct the test (< 10 ml). The gap is recommended to be chosen equal to 1 mm (Mezger, 2017). One of the main conditions in a rheological test is to choose the gap between the

448 plates larger than one fifth of the maximum grain diameter (Galli, 2016); therefore, the soil must be
449 sieved to 200 µm. The methodology consists on applying a shear rate to measure the rheological
450 parameters: viscosity and shear stress.

451 Similar to the slump test the first step consists on sample preparation. Three samples are prepared;
452 reference soil and two conditioned soil samples. Initially the soil is sieved at 200 µm, which reflects
453 72% of the soil weight percentage. The soil is then hydrated to reach a water content equal to 17%. At
454 this stage, the soil represents the first sample 'reference sample'. The second and third type of samples
455 to be tested are formed from the reference sample mixed with (i) foam A, generated at c_f = 1.5%,
456 FER=10, at FIR=60% and (ii) foam B, generated at c_f = 2%, FER = 8, at FIR = 60%, respectively.
457 These values represent the upper limit of the optimal foam parameters deduced from the slump tests.
458 The choice fell on these foam parameters since they produce low viscous conditioned soil paste; easier
459 to manipulate by the rheometer. The second step involves the rheological parameters measurements.
460 For that, each of the three prepared samples is placed in contact with the plate-plate system following
461 an increase in the shear rate from 1 to 500 s^{-1}. By the mean of the Peltier system, the temperature is
462 maintained to 20°C. Each test on conditioned soil is conducted twice. The mean variation of the
463 viscosity and shear rate in function of the yield stress are represented on Figure 13. Based on the
464 viscosity curves (Figure 13 (a)) the soil mixed with foams generated, each time, from foaming agent A
465 and B shows a viscosity decrease in comparison to the unconditioned soil viscosity. This observation
466 can be explained by the foam integration into the soil grains, reducing the interaction between the
467 grains and therefore decreasing its viscosity. In addition, the viscosity curves of soil conditioned with
468 both foams shows similar viscosity values, these results are in agreement with those deduced by the
469 slump tests that also showed similar flow behavior reflected by similar slump values.

470

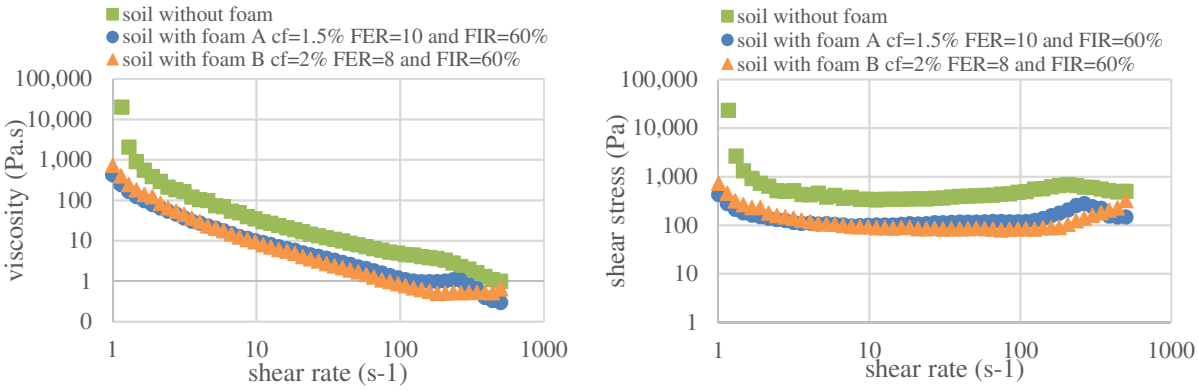

(a) (b)

Figure 13 : Soil with foam (a) viscosity curve (b) flow curve

The flow curves (Figure 13 (b)) are initiated by a decrease in the shear stress with the shear rate increase. This mechanism is observed in the case of clay, sand with foam (Galli, 2016) and can be related to the sample heterogeneity. In rheological measurements, the sample is usually supposed homogeneous and the local shear rate is derived from assuming that the globally imposed shear rate is distributed accordingly throughout the sample (Møller et al., 2006). In the case of this study, the sample is formed from real soil with high heterogeneity, which is identified on the flow curves by a decreased region corresponding to an unstable regime. Although this method of rheological measurement requires a low volume of material but it has limitation related to the inhomogeneous repartition of the shear stress in the sample. Galli (2016) initially used a CC27 with low volume of material and observed the decrease of the shear stress at the beginning of the shear rate increase. The researcher than used the ball measuring system that requires higher volume of material (500 ml) but gives satisfactory results of the flow and viscosity curves.

4.2 Microscopic analysis

The viscosity depends on the inner structure of the material, its outside forces and the ambient conditions. The objective of the microstructural analysis is to investigate the inner structure aiming to understand the effect of each foaming agent on the soil particles. As in the case of foam, the microscope Axio Imager M2m of ZEISS with image processing AxioVision software are used to perform and visualize the structure of the soil-foam samples. The tests are performed on two samples:

Sable de Beauchamp at it natural water content 17% conditioned with foaming agent A and B respectively, at the optimal foam parameters. The sample is then placed on a microscope lamella and subjected to transmission light allowing the observation of its inner structure. The microscopic observation are taken under a 100x optical zoom, sufficient to observe the structure. The initial photos taken are presented on Figure 14.

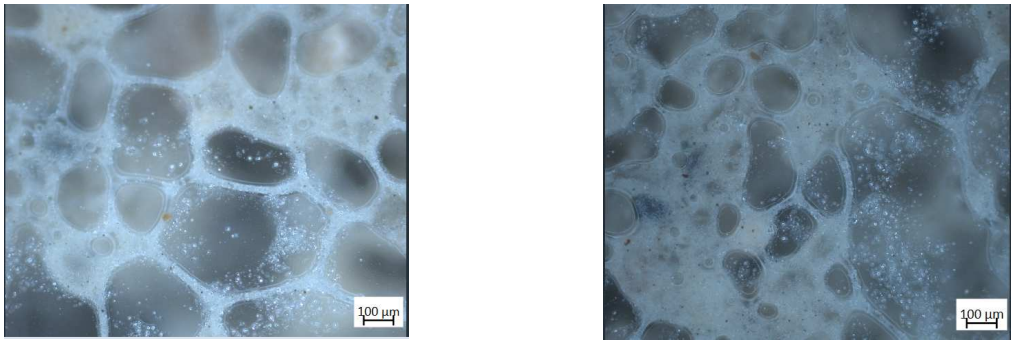

(a) (b)

Figure 14 : Conditioned soil SB microstructure: (a) with foam A, (b) with foam B

The photos clearly project the structure underlying the conditioned soil with foam. The foam is symbolized by air bubbles placed between the humid soil grains. The bubbles take an oval shape that does not allow following the foam bubbles diameters within the soil-foam mixture. A qualitative description of soil conditioning mechanism can be deduced as follow: The air bubbles integrate into the soil grains, spread out the particles and create a plastic sample. The density of grains is higher than water which squeeze the foam bubbles. In addition, the captured photos show that the bubbles in foam A are more evenly distributed into the soil while comparing them to the bubbles of foam B. Despite that, both tested conditioned soil samples have the same flow behavior manifested by the similar slump and viscosity, the foam bubbles repartition is not the same in the sample. Therefore, for the same type of soil, the repartition of the bubbles highly depends on the type of foam even for similar flow behavior. It should be recalled that the foam generated from foaming agent A is more fluid than foam generated from foaming agent B, which indicates that foam A integrates more easily into the soil structure, allowing to be homogeneously distributed.

5. Site approach

An additional advantage of this research is the ability to compare daily the laboratory results with the real excavation data of line 16-1 of Grand Paris Express project. This complex project is followed in details at each aspect. For some duration of time, the 6 EPBSs of several teams were working 24 h / 7 days. As mentioned above, the following up is possible to be conducted by the different teams, and not limited to the pilot, by the use of the TBM monitoring software where all the excavation data are saved. These collected data can be developed and analyzed in different ways. This section presents a first and general approach to analyze the excavation data. The target of the first part of the site approach is to describe the methodology adapted to choose the excavation parameters needed to achieve both objectives of the following parts. The second part aims to describe the strategy followed to recommend one foaming agent based on the excavation data analysis. The third part has as objective to compare the types and quantities of foaming agents deduced from the laboratory and used *in-situ*.

Choice of the excavation data

The foam data are saved in function of the three foam parameters 'c_f, FER, FIR' and as volume of foaming agent injected in 1 m^3 of excavated soil. Since each of the foam parameters used in the tunneling machines varies considerably in function of the ring number and given that the study aims to monitor the quantity of the foaming agent, the choice of the first set of parameters fell on following the volume of foaming agent injected in 1 m^3 of excavated soil. The second parameter to follow is a main concern, it should be chosen among a large list of parameters. As mentioned previously, one of the purposes of foam injection is to improve the flow behavior of the soil on the cutting wheel, which reduces the cutting wheel power and therefore increases the advance rate. Subsequently, the second set of parameters to choose, based on those affected by the foam injection, are cutting wheel torque, cutting wheel energy and advance rate. This analysis is not performed on the 6 EPBSs, only 3 are selected based on two requirements: (i) having the same diameter (ii) excavating more than 500 m in Sable de Beauchamp. Among these 3 EPBSs, the first one consumed foaming agent A while

536 excavating 980 m in Sable de Beauchamp and the other two EPBSs used foaming agent B with a total
537 drive of 800 m.

538 ***Recommendation of a foaming agent based on the excavation data analysis***

539 In order to recommend a foaming agent among two, the three mechanical parameters are presented in
540 function of foaming agent volume variation (Figure 13). The volume of foaming agent added is
541 significantly influenced not only by the FIR' but also by the c_f and FER. Therefore, the method
542 adapted represents a first approach to analyze the excavation data in function of the volume of
543 foaming agent. The target is to compare the effect of foaming agent on the soil in order to recommend
544 one. On Figure 15 (a), it can be noticed that the data are overlapped, yet divided into two sections; the
545 left one includes the largest number of rings where the foaming agent quantity varies between 0.4 and
546 0.9 l/m^3. The right region includes a small amount of rings with high foaming agent quantity (> 1 l/m^3)
547 which is explained by a highly clay soil. Table 2 resumes the values of chosen excavation parameters
548 in function of foaming agents A and B

549 *Table 2 : Values of excavation parameters in function of foaming agents A and B*

	Foaming agent A	Foaming agent B
Volume of foaming agent	0.75 ± 0.25	0.94 ± 0.3
Cutting wheel torque	5610 ± 610	5140 ± 960
Cutting wheel energy	21 ± 3	27 ± 7
Advance rate (mm/min)	49 ± 5	29 ± 8

550

551 In the case of the two EBPMs that use foaming agent B, the variation of the cutting wheel energy in
552 function of the foam volume quantity are presented on Figure 15 (b). It can be noticed that, contrary to
553 the precedent case, the values are distributed more widely and only one section is identified when
554 foaming agent B is used. Subsequently, in order to excavate the different drives, a different amount of
555 foaming agent is needed for the same type of soil. The injection of foaming agent A needs less foam
556 injection to maintain approximatively a similar torque with a lower energy and a higher advance rate.
557 Therefore, the foaming agent A is more efficient to excavate Sable de Beauchamp, in comparison with

the foaming agent B. The choice of the foam is consistent with the one deduced in the laboratory work.

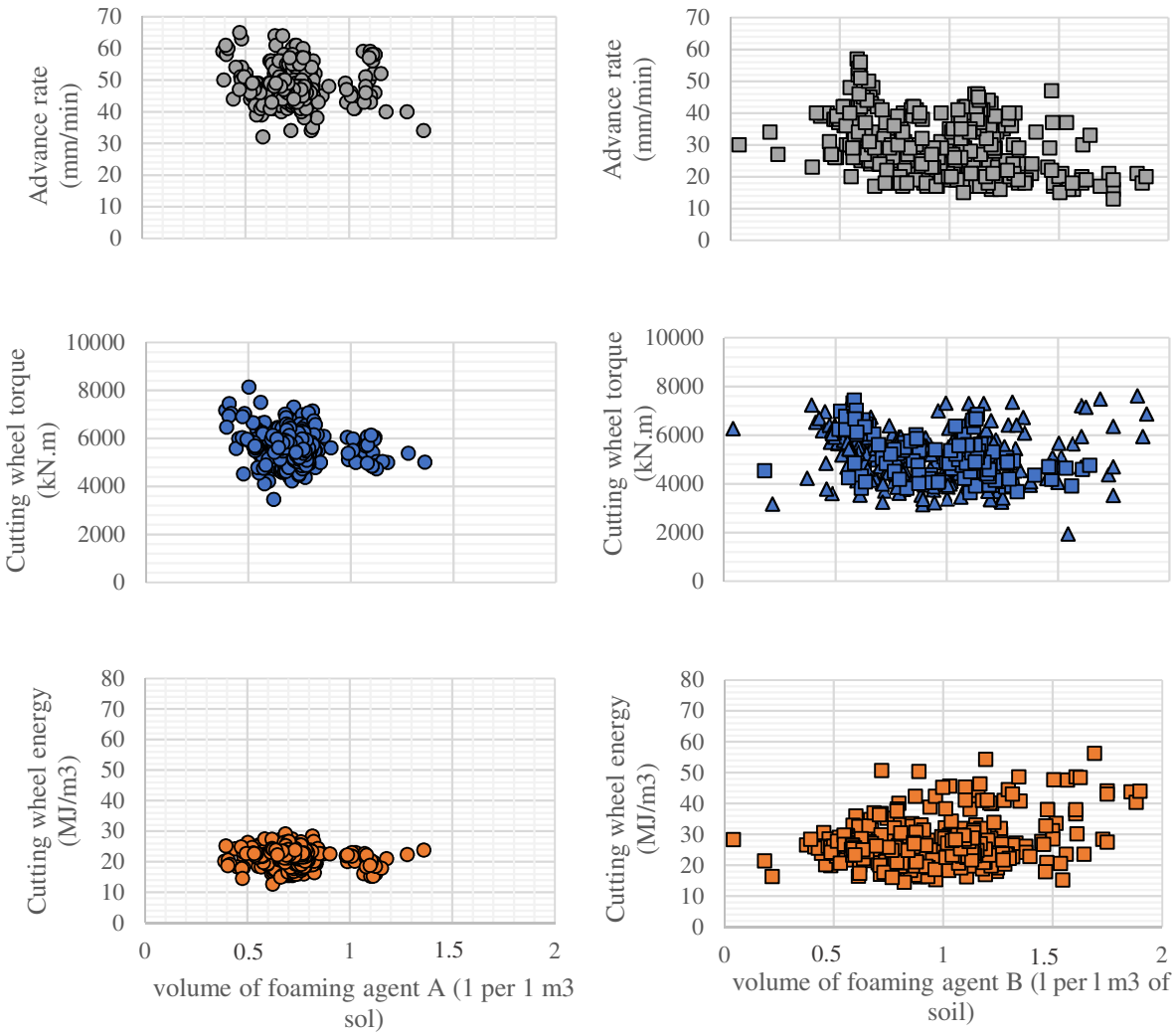

560 *Figure 15 : EPBS mechanical parameters variation in function of (a) volume of the foaming agent A,*
561 *(b) volume of the foaming agent B*

562

563 ***Comparison between the quantities of foaming agents, laboratory and in-situ***

564 Before comparing the recommendations of foaming agents deduced by the laboratory and by the in-
565 situ tests, one should keep in mind the difference between the initial conditions of the laboratory tests
566 and the EPBS functioning. The laboratory tests were performed at specific conditions. In the

567 laboratory, the foam generation, mixture and tests are performed under atmospheric pressure. On the
568 EPBS, the foam generation, injection with the soil and mixture in the excavation chamber are
569 performed under pressure. The texture of the soil-foam is in the excavation chamber also under
570 pressure.

571 The initial plan was to compare, for similar conditioned soil texture, the optimal foam quantities
572 deduced in paragraph 4 with the foam quantity used during soil excavation. In order to identify the
573 texture, a certain quantity of *in-situ* conditioned soil extracted from the screw conveyor, was collected
574 and subjected to a slump test. Unfortunately, it was not possible to go further in the initial plan since
575 the real conditioned soil samples were sticky and no bubbles were seen with the bare eye; the foam
576 bubbles have been deteriorated with time and under pressure extraction from the screw conveyor. For
577 this reason, the comparison between both results will not be limited to the mean quantities of foaming
578 agent but will be expanded to include their percentage of occurrence within the excavation drive and
579 the mechanical parameters values.

580 Firstly, to compare the *in-situ* foam data with the laboratory work, the optimal soil-foam parameters
581 deduced from this latter are represented in function of the Treatment Ratio (Tr) defined as volume of
582 foaming agent in l of 1 m^3 of soil, by the use of the equation (5). The equation (5) is deduced from
583 substitution of the foam parameters relationships while taken into account that the volume of *in-situ*
584 soil to be excavated equal to 1.

585 $$treatment\ ratio\ \left(l/m^3\right) = \ volume\ of\ foaming\ agent\ \left(l/m^3\right)$$

586 $$= c_f(\%) * 1\ (m^3) * FIR\ (\%)\ /\ (10 * FER) \qquad (5)$$

587 By applying equation (5), the optimal volume of foaming agent in l for 1 m^3 of soil can be deduced
588 from the laboratory work. This quantity mainly varies between 0.67 and 0.90 l/m^3 in the case of
589 foaming agent A that is larger than the quantity needed of foaming agent B, that varies between 1 to
590 1.5 l/m^3. Secondly, these quantities of foam recommended by the laboratory work and injected into the
591 EPBSs in function of their percentage of occurrence within the excavation drive, are presented on
592 Figure 16 and compared together. The interval of foaming agent quantities injected into the soil in the

tunneling machines is large, as the EPBS passes through several types of Sable de Beauchamp; from low to high quantity of clays with or without sandstone. The quantities of the soil with foam deduced from the laboratory research for foaming agent A fall into the interval of the injected foam quantities on the EPBS, that range between 0.6 and 0.9 l/m^3, giving a mean advance rate of the machine of 49 mm/min and a mean cutting wheel energy of 21 MJ/m^3. As for foaming agent B, it can be noticed that the volume of foam injected on the EPBSs, mainly varying between 0.4 and 1.2 l/m^3, falls partially into the optimal interval deduced by the laboratory work. This can be explained by the lower advance rate of the machine (29 mm/min) and the higher energy consumed (27 MJ/m^3) when using foaming agent B in comparison with foaming agent A. Consequently, based on both laboratory work and *in-situ* excavation data analysis, foaming agent A is recommended to be used when the EPB machine excavates into Sable de Beauchamp.

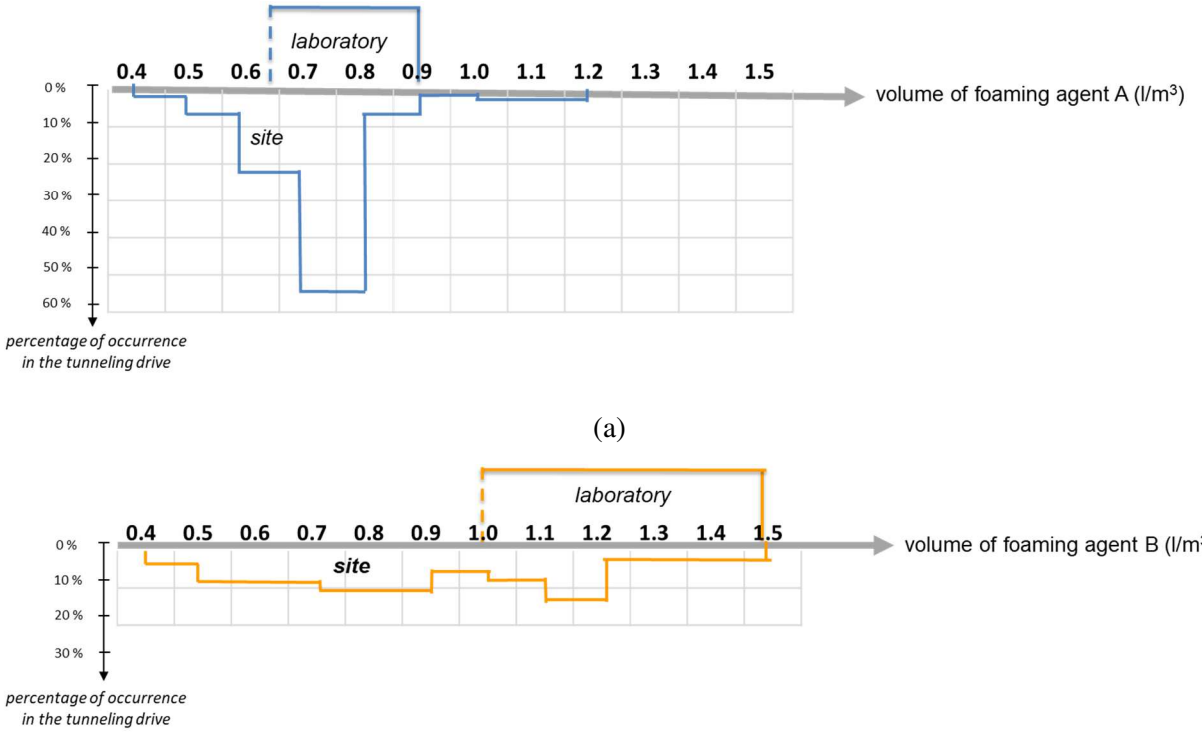

Figure 16 : Foaming agents quantity recommended and used (a) foaming agent A (b) foaming agent B

6. Discussions

A multiscale investigations consisting of micro, meso and macroscopic (real) scales are performed on foam and soil-foam mixtures. They allow to correlate between foam physical and chemical

608 characteristics, and to project them on the soil-foam tests results in order to deduce their effect on the
609 soil. Before going into details, one should mention that several main differences between both
610 laboratory test methods and the *in-situ* parameters challenge this study. As mentioned previously, the
611 laboratory tests use a high-speed stirrer to generate foam under atmospheric pressure. The quality of
612 the foam is therefore different than the one extracted from the in-situ foam generator. In addition, the
613 soil-foam mixture and tests are performed under atmospheric pressure, while all these mechanisms
614 occur under excavation pressure in the case of EPBS. The laboratory limited the investigation on
615 specific foam parameters while on the EPBS the foam parameters varies widely. The foam parameters
616 value difference also have a significant effect on the quality of foam, therefore on its quantity to inject
617 into the soil. Not to mention the scale effect between the laboratory and the excavation machine. At
618 the stage of this study, the recommendation of a foaming agent for sandy soil with silt is deduced. The
619 comparison of the quantities cannot be conclusive.

620 The relationships deduced in this research are summarized and interpreted within this paragraph.

621 ***Foam***

622 The micro investigations performed by the use of the microscope and the mesoscopic studies
623 conducted by the foam half-life measurements and the rheology tests, differentiate foam into two
624 categories:

625 Category I: foam based on surfactants and anti-clay polymers showing a medium stability, low
626 viscosity and bigger foam mean diameter as physical characteristics;

627 Category II: foam based on surfactants and polymer with lubrication effect. This category is
628 reflected by a foam with high stability and viscosity, and lower sized foam bubbles
629 percentage.

630 Both foam categories have common physical characteristics that are linked chemically to the presence
631 of the surfactants. These similarities are explained as followed:

- the surfactants are responsible of the thin film persisting between the foam bubbles cells independently of the foam stability category;
- both stability tests due to the gravity, performed on the two foams, show that the liquid drainage is generated initially and as result the foam volume degrades ;
- both flow behaviors follow a pseudo-plastic fluid mechanism: the foam evolves under shear rate destroying the bubbles and creating a more fluid texture.

Despite these similarities, the values of the physical characteristics of foams (half-life, viscosity and mean diameter of foam bubbles) are not identical. These differences can be explained by the following mechanisms:

- the presence of anti-clay polymer can be responsible on increasing the mean diameter of foam bubbles, therefore reducing the stability of the foam and its viscosity. ;
- the higher bubble size of foam decreases its stability; due to the gravity effect, the higher sized bubbles diameters produce a shorter path for liquid to drain;
- the correlation between the bubble size of foam and its viscosity is negative; higher sized bubbles tolerate smaller shear stress, in other terms they require a lower shear rate to break.

The previous works also showed that the polymer can have an effect on the characteristics of foam (Zhao et al., 2021; Li et al., 2022). Zhao et al. (2021) results show that the mean bubble radius decreases with the addition of anti-clay agents at 0 bar but increases at a pressure of 1 bar or 2 bar. The anti-clay agents weaken the stability of foam, and optimal concentrations of anti-clay agents for different test pressures proposed by Zhao et al. (2021).

Soil with foam

The meso scale, reflected by the slump and rheological tests conducted on conditioned soil with both foaming agents, show higher slump values and lower viscosity with optimal foam injections. These observations reflect the positive effect of the foam on the soil manifested by the flow improvement of the excavated material. This mechanism is related to the foam bubbles that insert the soil, slide between the grains, spread them out and hence create a pulpy compressible texture. However, the

quantity needed to obtain the same conditioned soil texture depends on the type of the foaming agent, the surfactant concentration and the foam expansion ratio. The meso scale results also showed that the slump of soil conditioned with foaming agent A is higher than that conditioned with foaming agent B at the same foam injection quantity. The foaming agent A is therefore recommended following the laboratory work. Based on the excavation data (macro scale), the injection of lower quantity of foaming agent A in comparison of foaming agent B in Sable de Beauchamp at a specific geological characteristics, show an improvement in the advance rate and a reduction of the energy. The foaming agent A is also recommended based on real excavation data. Recalling the characteristics of foaming agent A, it has medium stability with low viscosity. The medium foam stability is therefore sufficient for the sandy silt soil.

In order to understand the mechanism behind the variation in quantity between both foaming agents once mixed with soil, these observations are projected to the microscopic scale. The results show more evenly distributed bubbles in soil-foam matrix in the case of foam A in comparison to the foam B. Similar results were observed in the microstructure of foam alone. Therefore, the soil mixture with foam, changes the shape of the bubbles but not their characteristics. In addition, the microstructure of conditioned soil captured some large soil lumps that are related to the initial presence of clay particles into the soil that hindrance the effect of foam. In the case of the soil-foam B, this phenomenon is easily identified by the non-homogenous mixture observed by the microscope. Whereas, in the case of foaming agent A with smaller bubbles' diameter, the soil lumps are less detected. Consequently, when foam based on surfactants and polymers with lubrication effect (case of foaming agent B) is mixed with soil, it reduces the viscosity and enhances the workability of the mixture with no clay spreading. Whereas, in the case of foam generated from foaming agent A having surfactants and anti-clay polymer, the foam is able to enhance the workability of the mixture and to spread out the clay particles. Subsequently, one can distinguish between the role of the surfactants alone, from the role of surfactants combined with anti-clay polymer. The role of surfactant is purely related to the lubrication effect. This is not only shown on the flow behavior tests but it is also reflected on the real scale by the higher energy and lower advance rate. However, the anti-clay polymer changes the physical

685 characteristics of the foam by generating a homogeneous foam bubble with low viscosity able to easily
686 integrate the soil particles and separate those that can agglomerate together, resulting an excavation
687 with lower energy and higher advance rate.

688 7. Conclusions

689 This research reflects a three-level approach study: micro, meso and macro, performed on foam and
690 soil-foam mixtures. On the one hand, this analysis correlates between the physical characteristics of
691 foams and on the second hand, it explains their effects on soil conditioning. The soil is a sandy soil
692 with silt and the foam is based on surfactant with polymers (lubricant polymer or anti-clay polymer).
693 This article presents the methodology to adapt to correlate between the soil and foam physical
694 characteristics. Therefore the methodology presented can be applicable on other types of soil and
695 foams. The main conclusion at each of the three scales is the following:

696 - The micro study performed by the use of the microscope, deduces the role of each of the
697 surfactants and anti-clay polymers in the foam and the foam-soil matrix. The foam bubbles
698 can be generated with surfactants alone, once anti-clay polymers are added to the surfactants,
699 they monodisperse the foam bubbles and slightly increase their diameters. Once the foam is
700 mixed with soil, the anti-clay polymers conserve the monodispersed foam bubbles by
701 homogeneously dispersing the soil particles. ;
702 - These findings explained the meso results from the tests performed on foam and soil with
703 foam mixture by the use of the standard cone and rheometer respectively: a foam based on
704 surfactants and anti-clay agents with higher bubbles induced a less viscous foam with lower
705 stability in function of time. Once mixed with soil, the lower viscous foam with uniform
706 bubbles slips more easily into the soil and distributes homogenously the bubbles by dispersing
707 the clay, and therefore creating a pulpy homogeneous soil-foam mixture;
708 - The real (macro) study is the analysis of the excavation data. The results recommend the use
709 of foaming agent A over the foaming agent B, and confirm the confidence from the laboratory
710 tests (slump and rheology tests) as a key indicator to deduce the optimal soil-foam ratio.

711 The laboratory study is therefore able to highlight on the importance of the preliminary studies and to
712 promote their use by tunneling teams. It is not sufficient to perform only foam investigations or
713 conditioned soil tests, but performing both investigations and correlating between them are
714 recommended to compensate the soil heterogeneity. In the case when it is not possible to extract a
715 large quantity of soil, the properties of the soil retained from the core sample investigations combined
716 with the foam's physical characteristics can be used to deduce the most convenient foam to inject
717 within the soil.

718 8. Outlook

719

720 As for the future work, several condition of tests can be ameliorated, such as :

721 - studying the soil heterogeneity by increasing the mixtures between several types of soil
722 encountered on the TBM alignment such as mixtures between Sable de Beauchamp and Calcaire
723 Saint-Ouen (SO) or Marnes et Caillasses (MC). This way assures a larger comparison interval with
724 the *in-situ* data and allows to deduce the extent of the developed methodology.

725 - integrate the variation of the foam parameters c_f, FER and FIR in this study.

726 - analyzing the nano scale and molecular interactions between soil grains, water, surfactants and
727 polymers. The extension of the methodology to the molecular and nano scale allows a better
728 understanding the relationship between the soil and foam, which permits the tunnellers to develop
729 choose the foaming agent for each type of soil.

730 - study the long term characteristics of the excavated materials (hydro-mechanical and rheological
731 characteristics) allow their distribution in the adequate fields of valorization.

732 Declaration of Competing Interest

733 The authors declare that they have no known competing financial interests or personal relationships
734 that could have appeared to influence the work reported in this paper.

735

Acknowledgments

This research was found by 2018/0942 CIFRE agreement between ANRT, INSA Lyon and Eiffage Génie Civil, France in the framework of the PhD of Nour EL SOUWAISSI.

References

AFTES, GT4R3F1, 2000. Choix des techniques d'excavation mécanisée, Recommandations. Revue TOS, 157, 7–31.

ASTM C 143/C 143 M. 2015. Standard test method for slump of hydraulic-cement concrete.

Ball, R.P., Young, D.J., Isaacson, J., Champa, J., Gause, C., 2009. Research in soil conditioning for EPB tunnelling through difficult soils. In: Rapid Excavation and Tunneling Conference (RETC), Las Vegas, United States. 320–333.

Borio, L., Peila D., 2010. Study of the permeability of foam conditioned soils with laboratory tests. American Journal of Environmental Sciences, 6, 365–370. https://doi.org/10.3844/ajessp.2010.365.370

Boone, S. J., Artigiani, E., Shirlaw, J.N., Ginanneshi, R. Leinala, T., Kochmanova, N., 2005. Use of ground conditioning agents for earth pressure balance machine tunnelling. Tunnelling for a sustainable Europe : proceeding of an international congress pf Association Française des Travaux en Souterrain (AFTES) (Ed.), Spécifique, Lyon 2005, pp. 313–319. ISBN: 2951041667.

Budach, C., 2011. Untersuchungen zum erweiterten Einsatz von Erddruckschilden in grobkörnigem Lockergestein. Ph.D. thesis., Ruhr-Universität Bochum, 338 p.

Cantat, I., Cohen-Addad, S., Elias, F., Graner, F., Hôhler, R., Pitois O., Rouyer, F., Saint-Jalmes, A., 2010. Les mousses Structures et dynamiques. Belin editions.

Carigi, A., Todaro, C., Martinelli, D., Amoroso, C., Peila, D., 2020. Evaluation of the geo-mechanical properties property recovery in time of conditioned soil for EPB-TBM tunneling. Geosciences, 10, 438. https://doi.org/10.3390/geosciences10110438

De Oliveira, D.G.G., Thewes, M., Diederichs, M. S., 2019. Clogging and flow assessment of cohesive soils for EPB tunnelling: Proposed laboratory tests for soil characterisation. Tunnelling and Underground Space Technology, 94, 103110. https://doi.org/10.1016/j.tust.2019.103110

Djeran-Maigre, I., Dubujet, P., Vogel, TM., 2018. Variation over time of excavated soil properties treated with surfactants, Environmental Earth Sciences, 77 (3), 67. https://doi.org/10.1007/s12665-018-7230-z

Denkov, N., Tcholakova, S., Politova-Brinkova, N., 2020. Physicochemical control of foam properties. Colloid & Interface Science, 50, 101376. doi: 10.1016/j.cocis.2020.08.001

EFNARC, 2005. Specifications and guidelines for the use of specialist products for mechanized tunnelling (TBM) in soft ground and hard rock. Recommendation of European Federation of Producers and Contractors of Specialist Products for Structures, UK

El Souwaissi, N., Djeran-Maigre, I., Boulangé, L., Trottin, J.-L., 2020. Etudes au laboratoire et *in-situ* de l'effet d'agents moussants sur les sables de Beauchamp excavés au tunnelier à pression de terre. Journées Nationales de Géotechnique et de Géologie de l'Ingénieur, Lyon, France

Freimann, S., Galli, M., Thewes, M., 2018. Rheology of foam-conditioned sands: Transferring results from laboratory to real-world tunneling. Geotechnical Aspects of Underground Construction in Soft Ground – Negro & Cecilio Jr. (Eds), p. 145 - 151.

Galli, M., 2016. Rheological characterisation of Earth-Pressure-Balance (EPB) support medium composed of non-cohesive soils and foam. Ph.D. thesis, Ruhr-University Bochum, Germany

LCPC-SETRA, 2000. Réalisation des remblais et des couches de forme GTR_{2000}, $2^{ième}$ édition. SETRA, France

Guillermic, R.-M., 2011. Propriétés physico-chimiques des mousses : Études approfondies sur des mousses modèles et études exploratoires sur de nouvelles mousses. Ph.D. thesis, Université de Rennes, Rennes, France.

Hu, W., Rostami, J., 2021. Evaluating rheology of conditioned soil using commercially available surfactants (foam) for simulation of material flow through EPB machine. Tunnelling and Underground Space Technology incorporating Trenchless Technology Research, 112, 103881. https://doi.org/10.1016/j.tust.2021.103881

788 Huang, S., Wang, S., Xu, C. 2019. Effect of grain gradation on the permeability characteristics of
789 coarse-grained soil conditioned with foam for EPB Shield tunneling. KSCE Journal of Civil
790 Engineering, 23, 4662–4674. https://doi.org/10.1007/s12205-019-0717-7
791 Jancsecz, S., Krause, R., Langmaack, L., 1999. Advantages of soil conditioning in shield tunnelling:
792 experiences of LRTS Izmir. In: Alten, T. et al. (Eds.), Proceedings of International Congress on
793 Challenges for the 21st Century. Balkema, Rotterdam, 865– 875
794 Kim, T. H., Lee, I. M., Chung, H. Y., Park, J. J., Ryu, Y. M., 2021. Application Ranges of EPB Shield
795 TBM in Weathered Granite Soil: A Laboratory Scale Study. Applied Sciences, 11 (7), 2995.
796 https://doi.org/10.3390/app11072995
797 Li, S., Wan, Z., Zhao, S., Ma, P., Wang, M., Xiong, B. 2022. Soil Conditioning Tests on Sandy Soil
798 for Earth Pressure Balance Shield Tunneling and Field Applications. Tunnelling and Underground
799 Space Technology, vol. 120, article number 104271. https://doi.org/10.1016/j.tust.2021.104271.
800 Lovat, R., 2012. Mechanized Tunnelling in Soft Soil. General Aspects & History of Machine's
801 Development. Key note lecture, 71 p.
802 Martinelli, D., Winderholler, R., Peila, D., 2017. Undrained behaviour of granular soils conditioned for
803 EPB tunnelling – A new experimental procedure, Geomechanics and Tunnelling, vol. 10, n° 1, p.
804 81 - 89.
805 Mezger, T., 2017. Rhéologie appliquée. Anton Paar.
806 Milligan, G., 2000. Lubrication and soil conditioning in tunneling, Pipe Jacking and Microtunneling,
807 A State-of-the-Art Review. Geotechnical Consulting Group, G.W.E. Milligan.
808 Møller, P.C.F., Mewis, J., Bonn, D., 2006. Yield stress and thixotropy: on the difficulty of measuring
809 yield stress in practice. Soft Matter, 2, 274-283. https://doi.org/10.1039/B517840A
810 Peña, M.A., 2007. Foam as a soil conditioner in tunnelling: physical and mechanical properties of
811 conditioned sands. PhD thesis, University of Oxford, UK
812 Peila D., Oggeri C., Borio L., 2009. Using the slump test to assess the behavior of conditioned soil for
813 EPB tunneling. Environmental and Engineering Geoscience, 15 (3), 167–174.
814 https://doi.org/10.2113/gseegeosci.15.3.167

Peron, J.Y. and Marcheselli, P. 1994. Construction of the 'Passante Ferroviario' link in Milan, Italy, Lots 3P, 5P and 6P: Excavation by large earth pressure balanced shield with chemical foam injection. Proceedings Tunnelling 94, Institution of Mining and Metal lurgy, p. 679 – 707

Psomas, S., 2001. Properties of foam/sand mixtures for tunneling applications. Master's thesis, University of Oxford, Oxford, UK

Quebaud, S., 1996, Contribution à l'étude du percement de galeries par boucliers à pression de terre : amélioration du creusement par l'utilisation des produits moussants. PhD thesis, Université des Sciences et Technologies de Lille, Lille, France

Sebastiani, D., Vilardi, G., Bavasso, I., Di Palma, L., Miliziano, S. 2019. Classification of foam and foaming products for EPB mechanized tunnelling based on half-life time. Tunnelling and Underground Space Technology, 92, 103044. https://doi.org/10.1016/j.tust.2019.103044

Shin, Y. J., Kang, S. W., Lee, J. W., Kim, D. Y. 2021. Challenges of EPB TBM in Pressurized Mixed Grounds under Hangang River: Effect of Clogging. The 2021 World Congress on Advances in Structural Engineering and Mechanics (ASEM21) GECE, Seoul, Korea.

Tao, L., Chen, Z., Cui, J., Wang, H., Fang, Y. 2019. Experimental methods to assess the effectiveness of soil conditioning with foam in fully weathered granite. Advances in Materials Science and Engineering, 2019, 9046704. https://doi.org/10.1155/2019/9046704

Thewes, M. and Budach, C., 2010. Soil conditioning with foam during in EPB tunnelling. Gomechanisand Tunnelling, 3 (3), 256-267. https://doi.org/10.1002/geot.201000023

Thewes, M., Budach, C., Galli, M., 2010. Laboratory Tests with various conditioned soils for tunnelling with Earth Pressure Balance shield machines. In: Tunnel, n° 6, p. 21–30.

Vinai, R., Oggeri, C., Peila, D., 2008. Soil conditioning of sand for EPB applications: a laboratory research. Tunnelling and Underground Space Technology, 23 (3), 308–317. https://doi.org/10.1016/j.tust.2007.04.010

Vennekötter, J., 2012. Separationsfreier Mikrotunnelbau durch Pumpförderung schaumkonditionierter Böden. Ph.D. thesis, RWTH Aachen, Shaker, Aachen.

Wang, H., Wang, S., Zhong, J., Qu, T., Liu, Z., Xu, T., Liu, P., 2021. Undrained compressibility characteristics and pore pressure calculation model of foam-conditioned sand. Tunnelling and

843 Underground Space Technology incorporating Trenchless Technology Research, 118, 104161.
844 https://doi.org/10.1016/j.tust.2021.104161
845 Wei, Y., Yang, Y., Tao, M., Wang, D., Jie, Y., 2020. Earth pressure balance shield tunneling in sandy
846 gravel deposits: a case study of application of soil conditioning. Bulletin of Engineering Geology
847 and the Environment, 79, 5013–5030. https://doi.org/10.1007/s10064-020-01856-1
848 Williamson, G.E., Traylor, M.T., Higuchi, M., 1999. Soil conditioning for EPB shield tunneling on the
849 South Bay Ocean Outfall. In: Proceedings of RETC 1999, p. 897–925
850 Wu, Y., Mooney, M. A., and Cha, M., 2018. An experimental examination of foam stability under
851 pressure for EPB TBM tunneling**.** Tunnelling and Underground Space Technology, 77, 80-93.
852 https://doi.org/10.1016/j.tust.2018.02.011
853 Zhao, S., Li, S., Wan, Z., Wang, X., Wang, M., Yuan, C. 2021. Effects of anti-clay Agents on bubble
854 size distribution and stability of aqueous foam under pressure for Earth Pressure Balance Shield
855 Tunneling. Colloid and Interface Science Communications, vol. 42, article number 100424.
856 https://doi.org/10.1016/j.colcom.2021.100424.

Graphical abstract (without Author details)